Cellular/Molecular

PDP1ε Functions Downstream of the Circadian Oscillator to Mediate Behavioral Rhythms

Juliana Benito,[1]* **Hao Zheng,**[1,2]* **and Paul E. Hardin**[2]

[1]Department of Biology and Biochemistry, University of Houston, Houston, Texas 77204, and [2]Center for Research on Biological Clocks, Department of Biology, Texas A&M University, College Station, Texas 77843

The *Drosophila* circadian oscillator is composed of autoregulatory *period/timeless* (*per/tim*) and *Clock* (*Clk*) feedback loops that control rhythmic transcription. In the *Clk* loop, CLOCK-CYCLE heterodimers activate *vrille* (*vri*) and *PAR domain protein 1ε* (*Pdp1ε*) transcription, then sequential repression by VRI and activation by PDP1ε mediate rhythms in *Clk* transcription. Because VRI and PDP1ε bind the same regulatory element, the VRI/PDP1ε ratio is thought to control the level of *Clk* transcription. Thus, constant high or low PDP1ε levels in clock cells should eliminate *Clk* mRNA cycling and disrupt circadian oscillator function. Here we show that reducing PDP1ε levels in clock cells by ~70% via RNA interference or increasing PDP1ε levels by ~10-fold in clock cells does not alter *Clk* mRNA cycling or circadian oscillator function. However, constant low or high PDP1ε levels in clock cells disrupt locomotor activity rhythms despite persistent circadian oscillator function in brain pacemaker neurons that extend morphologically normal projections into the dorsal brain. These results demonstrate that the VRI/PDP1ε ratio neither controls *Clk* mRNA cycling nor circadian oscillator function and argue that PDP1ε is not essential for *Clk* activation. PDP1ε is nevertheless required for behavioral rhythmicity, which suggests that it functions to regulate oscillator output.

Key words: circadian rhythms; transcription regulation; feedback; *Drosophila*; behavior; biological clocks

Introduction

The *Drosophila* circadian timekeeping mechanism is composed of interlocked *period/timeless* (*per/tim*) and *Clock* (*Clk*) transcriptional feedback loops (Glossop et al., 1999). These feedback loops are initiated when CLOCK-CYCLE (CLK-CYC) binds E-boxes to activate *per*, *tim*, *vrille* (*vri*), and *PAR domain protein 1ε* (*Pdp1ε*) transcription around midday (for review, see Hardin, 2004, 2005). In the *per/tim* loop, *per* and *tim* mRNAs accumulate to high levels around dusk (Hardin et al., 1990; Sehgal et al., 1995), then PERIOD-TIMELESS (PER-TIM) heterodimers begin to accumulate in the nucleus around midnight and inhibit CLK-CYC binding to E-boxes (Hunter-Ensor et al., 1996; Myers et al., 1996; Darlington et al., 1998; Lee et al., 1999; Yu et al., 2006), thereby repressing *per* and *tim* transcription. After PER and TIM degradation during early morning, this inhibition is released, thus enabling another round of CLK-CYC-dependent transcriptional activation.

In the *Clk* loop, CLK-CYC represses *Clk* transcription indi-

rectly through VRI, which accumulates in parallel to its mRNA during the late day and binds V/P-boxes to repress *Clk* transcription (Cyran et al., 2003; Glossop et al., 2003). When PER-TIM inhibits CLK-CYC late at night, *vri* mRNA and protein levels fall and *Clk* repression is removed, thus promoting *Clk* activation. In addition to derepression by PER-TIM, *Clk* transcription is activated by PDP1ε (Cyran et al., 2003). PDP1ε is one of eight tissue-specific PDP1 isoforms that arise via alternative splicing (Reddy et al., 2000; Grumbling and Strelets, 2006). Loss of *Pdp1* leads to developmental lethality, with few *Pdp1*[P205] null mutant animals surviving to the pupal stage (Cyran et al., 2003). In clock cells, *Pdp1ε* mRNA and protein do not accumulate to high levels until late at night (Cyran et al., 2003). Because PDP1ε levels rise above those of VRI, PDP1ε is thought to displace VRI on V/P-boxes to activate *Clk* transcription (Cyran et al., 2003). However, *Clk* mRNA is expressed at peak levels in *Clk*[Jrk] and *cyc*[01] mutants (Glossop et al., 1999), suggesting that *Clk* can be activated independently of PDP1ε. This result contrasts with the loss of *Clk* expression in *Pdp1*[P205] larvae (Cyran et al., 2003), although it is possible that loss of all PDP1 isoforms causes developmental defects that alter clock cell fate or function, thus indirectly eliminating *Clk* expression.

If *Clk* mRNA cycling is driven by competition between PDP1ε and VRI for V/P-box binding, then reducing or increasing PDP1ε expression in clock cells should disrupt *Clk* mRNA cycling and, consequently, circadian oscillator function. Here we use the Gal4/UAS system to drastically reduce (via RNA interference) or increase PDP1ε levels in oscillator cells. Constant low or high PDP1ε levels had little effect on *Clk* mRNA cycling and abundance, thus demonstrating that the VRI/PDP1ε ratio does

not regulate *Clk* mRNA rhythms or circadian oscillator function. However, constant low or high PDP1ε levels drastically reduced behavioral rhythmicity even though oscillator function persists in pacemaker cells that drive rhythmic behavior. These data demonstrate that PDP1ε is not an essential component of the circadian oscillator, but rather functions to mediate circadian clock output.

Materials and Methods

PDP1ε antibody generation. Full-length PDP1ε was expressed in *Escherichia coli*, purified, and used to produce antisera in guinea pigs. pET28a(+) vector was initially modified to contain an *Spe*I site by inserting the duplexed Na and Ns oligonucleotides (Na, 5′-GATCCATAC-TAGTACACGAATTCGTATCCGACGACA-3′; Ns, 5′-TATGTCGTC-GGATACGAATTCGTGTACTAGTATG-3′) at the *Nde*I and *Bam*HI sites. An ∼2.4 kb *Spe*I–*Xho*I fragment from *Pdp1ε* cDNA clone CG27708 was inserted into the modified pET28a(+) vector to generate pET28a(+)–*Pdp1ε*, which expresses an N-terminal HIS-tagged PDP1ε fusion protein that contains the entire coding sequence of PDP1ε. pET28a(+)–*Pdp1ε* was transformed into BL21 cells, and protein expression was induced using isopropyl β-D-1-thiogalactopyranoside. PDP1ε fusion protein was purified from cell lysates using a nickel affinity column (GE Healthcare, Piscataway, NJ) as described previously (Houl et al., 2006). A single band at the predicted molecular weight of the PDP1ε fusion protein (∼75 kDa) was detected and used to immunize guinea pigs for antibody production (Cocalico Biological, Reamstown, PA). Although the newly generated PDP1 antibody is capable of detecting all eight isoforms of PDP1, PDP1ε is specifically targeted in clock neurons because this PDP1 isoform is uniquely expressed in the CNS (Reddy et al., 2000; Grumbling and Strelets, 2006) and is eliminated in *Clk*^{Jrk} and *cyc*^{01} mutant flies (see Fig. 1*A*,*B*).

Western blotting. The VRI antibody was described previously (Glossop et al., 2003). VRI and PDP1ε were detected on 7.5% polyacrylamide gels. For both antibodies, primary antibodies were used at a dilution of 1:5000 with horseradish peroxidase-conjugated goat anti-guinea pig (Sigma, St. Louis, MO) secondary antibody diluted 1:1000. The relative levels of PDP1ε and VRI were quantified as the ratio of PDP1ε or VRI band intensity to that of a nonspecific background band using Quantity One 1-D Analysis software (Bio-Rad, Hercules, CA). These relative VRI levels were normalized to VRI levels in *w*^{1118} at Zeitgeber time 17 (ZT17) or ZT15 on each blot to obtain the final levels of VRI.

Fly stocks and transgenic flies. The wild-type (Canton-S), *w* (*w*^{1118}), *cyc*^{01}, *per*^{01}, *tim*Gal4, and *pdf*Gal4 strains have been described previously (Konopka and Benzer, 1971; Hazelrigg et al., 1984; Emery et al., 1998; Rutila et al., 1998; Park et al., 2000). The UAS-PDP1i transgene was constructed as follows. *Pdp1* genomic (1200 bp) and cDNA (400 bp) fragments comprising exons 5, 6, and first part of exon 7 were amplified by PCR using primers having unique 5′ restriction sites. Primers used for the genomic fragment were 5′-GAATTCCTGATGGCCTGCCC-GGCACGCATCTGG-3′ and 5′-GCGGCCGCATTCTGAGCGGA-AT-AAATTTGG-3′, in which the underlined sequences correspond to *Eco*RI and *Not*I sites, respectively. Primers used for the cDNA fragment were 5′-GCGGCCGCATTTTCCTTCTCCAAGTAGCGTGC-3′ and 5′-GGTACCCTGATGGCCTGCCCGGCACGCATCTGG-3′, in which the underlined sequences correspond to *Not*I and *Kpn*I sites, respectively. When choosing the cDNA fragment for the inverted sequence, special care was taken to avoid splice donor sequences. The cDNA fragment was fused to the genomic fragment in an inverted orientation just after the exon 7 splice acceptor to disrupt direct repeats. Each PCR fragment was gel purified, ligated into pCR-XL-TOPO (Invitrogen, Carlsbad, CA), and transformed following the manufacturer's instructions. Clones were sequenced, and subsequently, the genomic PCR product was excised from pCR-XL-TOPO as an *Eco*RI–*Not*I fragment and cloned into the *Eco*RI and *Not*I sites of pUAST to form UAS-*Pdp1ε*GEN. The cDNA fragment was excised using *Not*I and *Kpn*I and ligated into the *Not*I and *Kpn*I sites of UAS-*Pdp1ε*GEN to form UAS-PDP1i.

To construct the UAS-*pdp1ε* transgene, *Pdp1ε* cDNA clone GH27708 was digested with *Avr*II and *Bsu* 36I; the resulting fragment was blunted

using Klenow and inserted in pBS KS at the *Eco*RV site to form pBS-*Pdp1ε*. The *Pdp1ε* cDNA fragment was excised from pBS-*Pdp1ε* using *Xho*I and *Not*I and inserted into *Xho*I and *Not*I digested pUAST (Brand and Perrimon, 1993) to form UAS-PDP1ε.

The UAS-PDP1i and UAS-PDP1ε transgenes were used to generate transgenic flies via P-element-mediated transformation. At least five independent lines were generated for each transgene. Flies with inserts on the second and third chromosome were balanced using In(2LR)CyO or In(3LR)TM6B, respectively. All fly strains were reared on medium containing corn meal, molasses, yeast, agar, and Tegosept (a mold inhibitor) at 25°C.

RNA quantification. *Clk* mRNA levels were assayed by quantitative real-time PCR (qPCR). Flies were entrained in a 12 h light/dark (LD) cycle for at least 3 d, collected every 4 h, and immediately stored at −80°C. Total RNA was isolated from fly heads using TRIZOL (Invitrogen) or the ToTALLY RNA kit (Ambion, Austin, TX). To eliminate genomic DNA contamination, each sample was treated with DNase (Promega, Madison, WI). First-strand cDNA was synthesized from 1 μg of RNA using random primers and Superscript II (Invitrogen). For qPCR, TaqMan assays were performed using the following *Clk* primers and probes: forward primer, 5′-GCGTCCCGCTTCGAGTT-3′; reverse primer, 5′-TGGCCTTCGGCGATATTC-3′; probe 6FAM-TGGCA-ATATCAGCTCCACA-MGBNFQ. Ribosomal protein 49 (RP49) was used as the internal loading control. The primers and TaqMan probe for RP49 were as follows: forward primer, 5′-CTGCCCACCGGATTCAAG-3′; reverse primer, 5′-CGATCTCGCCGCAGTAAAC-3′; probe VIC-CCTCCAGCTCGCGCACGTTG-MGBNFQ. Reactions were run on an Applied Biosystems (Foster City, CA) Prism 7000. The relative levels of *Clk* and RP49 RNAs were calculated based on standard curves for *Clk* and RP49 that were run in each assay. *Clk* levels were normalized to RP49 at each time point.

Brain whole-mount immunofluorescence. Flies were entrained in LD cycles for at least 3 d and kept in constant darkness (DD). On the second day of DD, transheterozygous UAS-PDP1i+*tim*Gal4 and control *w* flies were collected at circadian time 9 (CT9) and CT21, and their brains were dissected in 1× PBS, pH 7.4. Brains were fixed with 3.7% formaldehyde for 15 min at room temperature, followed by two washes with 1× PBS and one wash with PBT (1× PBS, pH 7.4, and 0.5% Triton X-100). Brains were then incubated with 5% goat serum in PBT for 3 h at room temperature to reduce nonspecific immunoreactivity. Primary antibodies were diluted in PBT plus 2% goat serum and incubated with samples at 4°C for 48 h. The primary antibodies used were rabbit polyclonal anti-pigment dispersing factor (PDF) (diluted 1:1000; kindly provided by Dr. A. Sehgal, University of Pennsylvania Medical School, Philadelphia, PA) and rat polyclonal anti-TIM (diluted 1:800; kindly provided by Dr. M. W. Young, Rockefeller University, New York, NY). Brains were then equilibrated to room temperature for 2 h and washed with PBT for 30 min six times at room temperature. Specimens were incubated overnight with fluorescently labeled secondary antibodies diluted 1:200 in PBT at 4°C. The secondary antibodies used were Cy3-conjugated goat anti-rabbit (Jackson ImmunoResearch, West Grove, PA) for anti-PDF and Alexa 488-conjugated goat anti-rat (Invitrogen, Eugene, OR) for anti-TIM. Brains were equilibrated to room temperature for 2 h, washed with PBT for 30 min six times at room temperature, and mounted on glass slides using Vectashield (Vector Laboratories, Burlingame, CA). This procedure was also used for immunostaining UAS-PDP1i+*tim*Gal4 and control UAS-PDP1i flies, except flies were collected at ZT9 and ZT21; PDP1 antiserum was diluted 1:30,000; and PDP1 was detected using an Alexa 488-conjugated goat anti-guinea pig secondary antibody (Invitrogen).

A similar protocol was used to analyze transheterozygous UAS-PDP1ε+*tim*Gal4 and control UAS-PDP1ε flies with the following changes: flies were collected at CT1 and CT13 on the second day of DD; PBT was replaced by PAXD (5% BSA, 0.3% Triton X-100, and 0.3% sodium deoxycholate); primary antibodies were incubated overnight and washed for 1 h six times; the primary antibodies were rabbit polyclonal anti-PER (diluted 1:15,000; a gift from J. Hall, Brandeis University, Waltham, MA) and guinea pig anti-PAP (diluted 1:1000; a gift from P. Taghert, Washington University, St. Louis, MO) (to detect PDF); secondary antibodies were incubated overnight at 4°C and washed for 1 h six
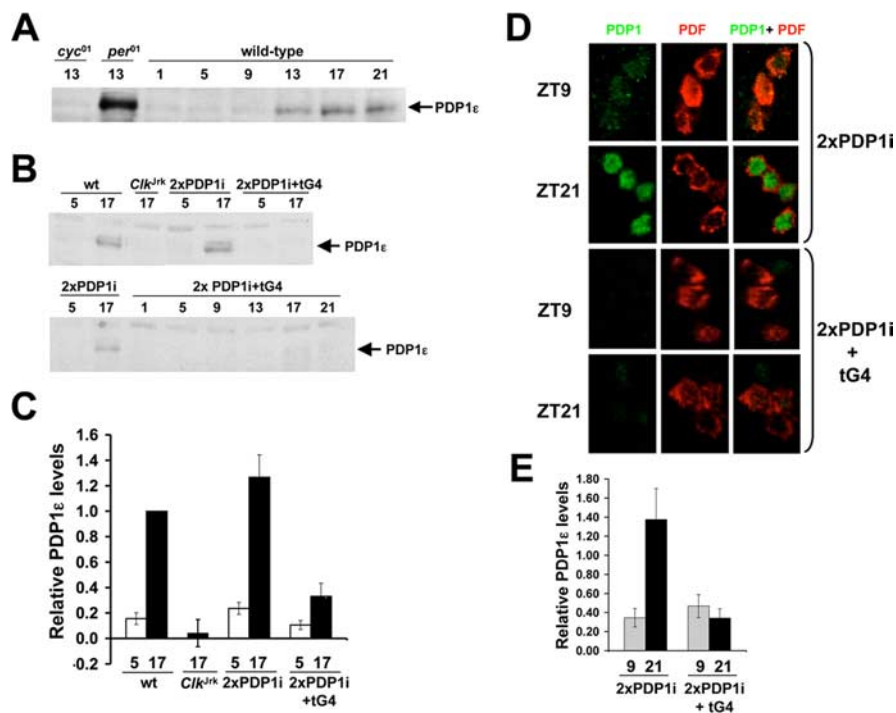
Figure 1. RNAi directed against PDP1 effectively reduces PDP1ε levels. **A**, Western blot of head extracts from *cyc*[01], *per*[01], and wild-type flies collected at the indicated times under LD conditions and probed with PDP1 antibody. **B**, Western blots containing head extracts from wild-type (wt), *Clk*[Jrk], w;UAS-PDP1i/+;UAS-PDP1i/+ (2xPDP1i), and w;UAS-PDP1i/+;UAS-PDP1i/*tim*Gal4 (2xPDP1i+tG4) flies (top) or 2xPDP1i and 2xPDP1i+tG4 flies (bottom) collected at the indicated times under LD conditions and probed with PDP1 antibody. The Western blot at the top contains a different transheterozygous combination of 2xUAS-PDP1i transgenes than that at the bottom. **C**, Quantification of PDP1ε levels in **B** and at least two independent repeats of each transheterozygous combination. PDP1ε levels were quantified as described in Materials and Methods. **D**, Brains dissected from 2xPDP1i+tG4 and control 2xPDP1i flies collected at ZT9 and ZT21 were probed with PDP1 and PDF antibodies. A representative 1 μm optical section of sLNvs is visualized for PDP1 (left panels), PDF (middle panels), or PDP1 plus PDF (right panels). **E**, PDP1 immunostaining in 2xPDP1i+tG4 and control 2xPDP1i flies was quantified as the ratio of PDP1/PDF staining. Staining in sLNvs was quantified from at least nine brains (i.e., at least 3 brains from 3 independent experiments).

times; and the secondary antibodies used were Alexa 488-conjugated goat anti-rabbit (to detect PER) and Cy3-conjugated goat anti-guinea pig (to detect PDF). This procedure was also used for immunostaining UAS-PDP1ε+*tim*Gal4 and control UAS-PDP1ε flies, except flies were collected at ZT9 and ZT21; PDP1 antiserum was diluted 1:30,000; PDP1 was detected using an Alexa 488-conjugated goat anti-guinea pig secondary antibody (Invitrogen); and rabbit polyclonal anti-PDF (kindly provided by Dr. A. Sehgal) was used to detect PDF.

Immunostaining in brains was visualized on an Olympus (Tokyo, Japan) FV1000 confocal microscope. Serial Z-stack images were obtained at 1 μm intervals using a 60× objective. Images were processed using Photoshop (Adobe Systems, San Jose, CA). Immunofluorescence was quantified in the LNvs using NIH Image J (version 1.33u; Wayne Rasband, freely available at http://rsb.info.nih.gov/ij/). Briefly, for each group of neurons, mean pixel intensity was calculated for the green (TIM, PER, or PDP1) and red (PDF) channels, respectively. TIM, PER, or PDP1 immunofluorescence was expressed as a ratio of TIM/PDF, PER/PDF, or PDP1/PDF mean pixel intensity, respectively.

To visualize projections from sLNvs and lLNvs, brains were dissected from flies collected at ZT21, fixed with 5% paraformaldehyde for 30 min, and incubated with a 1:800 dilution of rabbit polyclonal anti-PDF for 48 h at 4°C. Brains were then washed in PBT six times for 30 min, incubated in a 1:200 dilution of Cy3-conjugated anti-rabbit secondary antibody for 24 h at 4°C, and washed again in 1× PBST six times for 30 min before being visualized on an Olympus FV1000 confocal microscope. Serial Z-stack images were obtained at 2.5 μm intervals using a 20× objective. Images were processed using Photoshop (Adobe Systems).

Analysis of behavioral rhythms. Locomotor activity of adult male w,

transheterozygous UAS-PDP1i, transheterozygous UAS-PDP1i+*tim*Gal4, transheterozygous UAS-PDP1i+*pdf*Gal4, transheterozygous UAS-PDP1ε, transheterozygous UAS-PDP1ε+*tim*Gal4, and transheterozygous UAS-PDP1ε+*pdf*Gal4 flies that were <3 d old were monitored as described previously (Tanoue et al., 2004). Briefly, flies were entrained in LD cycles at 25°C for 3 d and transferred into DD. Locomotor activity behavior was monitored continuously during entrainment and for at least 7 d in DD using *Drosophila* activity monitors (Trikinetics, Waltham, MA). Data collected during DD were subjected to periodogram analysis using the Fly Activity Analysis Suite for Mac OSX (FaasX, version 0.7.1, copyright 2002–2003; M. Boudinot, Centre National de la Recherche Scientifique-Institut Neurobiologie Alfred Fessard, Gif sur Yvette, France). Flies with a power ≥10 and a width ≥2 in periodogram analysis were designated as rhythmic. Activity was calculated as the number of activity events occurring every 30 min.

Results
Constant low PDP1ε levels do not disrupt *Clk* mRNA cycling or oscillator function
Because VRI-dependent repression and PDP1ε-dependent activation are thought to control *Clk* mRNA cycling, we hypothesized that lowering PDP1ε levels would disrupt *Clk* mRNA cycling by reducing *Clk* mRNA levels and/or increasing the proportion of the cycle that *Clk* is at trough levels. To test this hypothesis, we used the UAS/GAL4 system to inhibit PDP1 expression in clock cells via RNA interference. A PDP1 RNA interference transgene (UAS-PDP1i) was generated and driven in clock cells by *tim*Gal4. Flies bearing both the UAS-PDP1i and *tim*Gal4 transgenes, which we will refer to as UAS-PDP1i+*tim*Gal4, were entrained in LD cycles along with UAS-PDP1i- and w-positive control and *Clk*[Jrk]-negative control flies, collected at times when PDP1ε levels are high (ZT17, where ZT 0 refers to lights on and ZT12 refers to lights off during LD) or low (ZT5) in wild-type flies (Cyran et al., 2003), and used to prepare head extracts for Western blot analysis. Western blot analyses were probed with a newly generated antibody that detects PDP1ε based on the following criteria: it recognizes a ~80 kDa protein that is rhythmically expressed with a peak around ZT17–ZT21, it is absent in *Clk*[Jrk] and *cyc*[01] flies, and it is at high levels in *per*[01] flies (Cyran et al., 2003) (Fig. 1*A*,*B*). Flies with transheterozygous UAS-PDP1i inserts driven by *tim*Gal4, which we will refer to as 2xPDP1i+*tim*Gal4, reduce PDP1ε levels to ~25–30% of control 2xPDP1i and w values at ZT17, which is close to normal PDP1ε trough levels (Fig. 1*B*,*C*). These low levels of PDP1ε are not attributable to a phase shift in 2xUAS-PDP1i+*tim*Gal4 flies because PDP1ε remains at low levels in head extracts from 2xPDP1i+*tim*Gal4 flies collected every 4 h (Fig. 1*B*). These results establish that RNA interference directed against *Pdp1* effectively inhibits PDP1ε expression in heads from 2xUAS-PDP1i+*tim*Gal4 flies.

Because >80% of clock gene expression in fly heads emanates from photoreceptors (Glossop and Hardin, 2002), we wanted to determine whether low levels of PDP1ε are also seen in brain

pacemaker neurons from 2xPDP1i+ *tim*Gal4 flies. 2xPDP1i+*tim*Gal4 and control 2xPDP1i flies were entrained in LD cycles and collected at times when PDP1ε levels are high (ZT21) or low (ZT9). Brains from these flies were dissected, probed with antisera against PDP1ε and the LN_v marker PDF, and imaged via confocal microscopy. In brains from 2xPDP1i flies, the intensity of PDP1ε immunofluorescence in LN_vs was high at ZT21 and low at ZT9, whereas the intensity of PDP1ε immunofluorescence in LN_vs from 2xPDP1i+*tim*Gal4 brains remained low at both ZT21 and ZT9 (Fig. 1*D*,*E*). These results demonstrate that RNA interference directed against *Pdp1* effectively inhibits PDP1ε expression in LN_vs from 2xUAS-PDP1i+*tim*Gal4 flies.

To determine whether low levels of PDP1ε disrupt *Clk* mRNA cycling, we entrained 2xUAS-PDP1i+*tim*Gal4 and control *tim*Gal4 flies, collected them every 4 h starting at ZT1, and extracted head mRNA for qPCR analysis. *Clk* mRNA in 2xUAS-PDP1i+*tim*Gal4 flies cycled with an approximate fivefold amplitude (Fig. 2*A*), which is similar to that in *tim*Gal4 control (Fig. 2) and wild-type flies (Bae et al., 1998; Darlington et al., 1998). *Clk* mRNA was also measured in 2xUAS-PDP1i flies; however, an ~10-fold *Clk* mRNA cycling was seen (data not shown), mainly because of anomalously high peak levels. The waveform of *Clk* mRNA cycling in 2xUAS-PDP1i+*tim*Gal4 and control *tim*Gal4 flies was similar, with *Clk* mRNA accumulating to peak levels around dawn and falling to trough levels around dusk (Fig. 2*A*). Just after dawn, *Clk* mRNA levels in 2xUAS-PDP1i+*tim*Gal4 flies are somewhat lower than in control *tim*Gal4 flies, which might suggest some effect of PDP1ε in lowering *Clk* mRNA levels at this time. Nevertheless, these results demonstrate that reduced PDP1ε levels have relatively little effect on *Clk* mRNA cycling amplitude and waveform.

The approximate fivefold cycling of *Clk* mRNA in 2xUAS-PDP1i+*tim*Gal4 flies suggests that the circadian feedback loops are functioning normally. Because VRI functions to repress *Clk* transcription, we would expect to see high-amplitude VRI cycling that is antiphase to that of *Clk* mRNA (Cyran et al., 2003; Glossop et al., 2003). Indeed, VRI levels increase as *Clk* mRNA levels decrease, and *Clk* mRNA levels increase as VRI levels decrease in 2xUAS-PDP1i+*tim*Gal4 flies (Fig. 2*B*,*C*). This result is consistent with the role of VRI as a *Clk* repressor and provides further confirmation that the circadian feedback loop is functional in 2xUAS-PDP1i+*tim*Gal4 flies. The high VRI/PDP1ε ratio in 2xUAS-PDP1i+*tim*Gal4 flies would predict that *Clk* mRNA should be quite low, yet *Clk* mRNA levels and cycling are not appreciably altered. This result indicates that VRI/PDP1ε ratio does not control *Clk* mRNA cycling and argues that *Clk* may be activated by factors other than PDP1ε.

Constant high PDP1ε levels do not disrupt *Clk* mRNA cycling or oscillator function
If PDP1ε activates *Clk* transcription, we would expect that constant high levels of PDP1ε would decrease the VRI/PDP1ε ratio, resulting in higher *Clk* mRNA levels and a reduced *Clk* mRNA cycling amplitude. To determine whether this is the case, we used
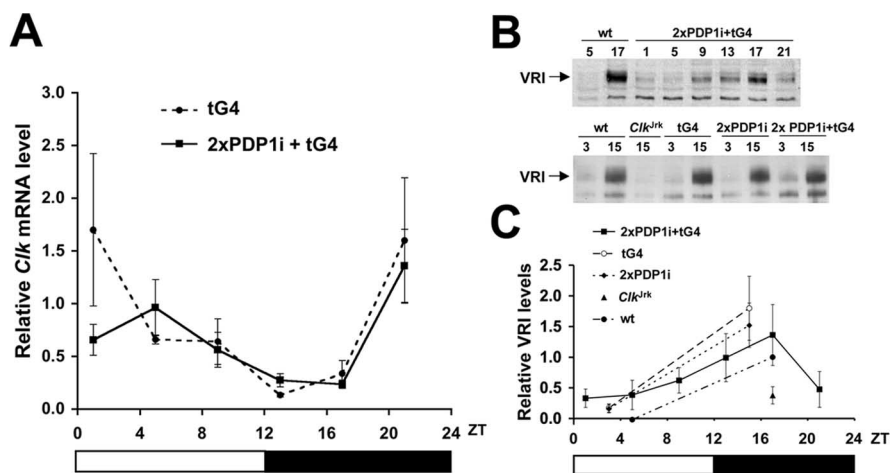

Figure 2. Constant low PDP1ε levels do not disrupt *Clk* mRNA or VRI cycling. *A*, qPCR of *Clk* mRNA from the heads of *w;+/+;timGal4/+* (*tim*Gal4) and *w;UAS-PDP1i/+;UAS-PDP1i/timGal4* (2xPDP1i+tG4) flies collected at the indicated times under LD conditions (ZT). Relative *Clk* mRNA levels were quantified as described in Materials and Methods. The black and white bars represent times when lights were on or off, respectively. *B*, Western blots of head extracts from 2xPDP1i+tG4 and wild-type, *Clk*^Jrk, *tim*Gal4 (tG4), and *w;UAS-PDP1i/+;UAS-PDP1i/+* (2xPDP1i) control flies collected at the indicated times under LD conditions and probed with VRI antibody. *C*, Quantification of VRI levels from the Western blots in *B* and at least two independent repeats. VRI levels were quantified as described in Materials and Methods and normalized to wild type at ZT17. wt, Wild type.

the UAS/GAL4 system to overexpress PDP1ε in clock cells. A UAS-PDP1ε transgene was constructed and driven in clock cells by *tim*Gal4. Flies containing both the UAS-PDP1ε and *tim*Gal4 transgenes, which we will refer to as UPDP1ε+*tim*Gal4 flies, were entrained in LD cycles along with control flies containing the UAS-PDP1ε insert only (UPDP1ε), collected every 6 h during LD starting at ZT3, and used to prepare head extracts for Western blot analysis. Flies with two different UPDP1ε inserts driven by *tim*Gal4 have between 5- and 20-fold higher levels of PDP1ε compared with control UPDP1ε flies, depending on the time point (Fig. 3*A*,*B*), demonstrating that UPDP1ε+*tim*Gal4 flies do indeed overexpress PDP1ε in fly heads.

To determine whether UPDP1ε+*tim*Gal4 flies also produce high levels of PDP1ε in brain pacemaker neurons, UPDP1ε+*tim*Gal4 and UPDP1ε control flies were entrained in LD cycles and collected at times when PDP1ε levels are high (ZT21) or low (ZT9). Brains from these flies were dissected, probed with PDP1ε and PDF antisera, and imaged via confocal microscopy. In brains from UPDP1ε flies, the intensity of PDP1ε immunofluorescence was high at ZT21 and low at ZT9 in LN_vs, whereas the intensity of PDP1ε immunofluorescence in LN_vs from UPDP1ε+*tim*Gal4 brains remained high at both ZT21 and ZT9 (Fig. 3*C*,*D*). Thus, consistent with results in whole heads, PDP1ε expression is constantly high in LN_vs of UPDP1ε+*tim*Gal4 flies.

To determine whether high levels of PDP1ε disrupt *Clk* mRNA cycling, we entrained UPDP1ε+*tim*Gal4 flies and control UPDP1ε flies in LD, collected them every 4 h starting at ZT1, and extracted head mRNA for qPCR analysis. The overall levels of *Clk* mRNA in UPDP1ε+*tim*Gal4 flies were comparable to those in control UPDP1ε flies (Fig. 4*A*). The phase of *Clk* mRNA cycling was also similar in UPDP1ε+*tim*Gal4 and control UPDP1ε flies in that the peak was somewhat variable (i.e., between ZT21 and ZT5 depending on the strain) and the trough was at ZT13 (Fig. 4*A*). From these results, it is apparent that high levels of PDP1ε neither increased the overall levels of *Clk* mRNA nor broadened the *Clk* mRNA peak, indicating that the VRI/PDP1ε ratio does not control *Clk* mRNA cycling.

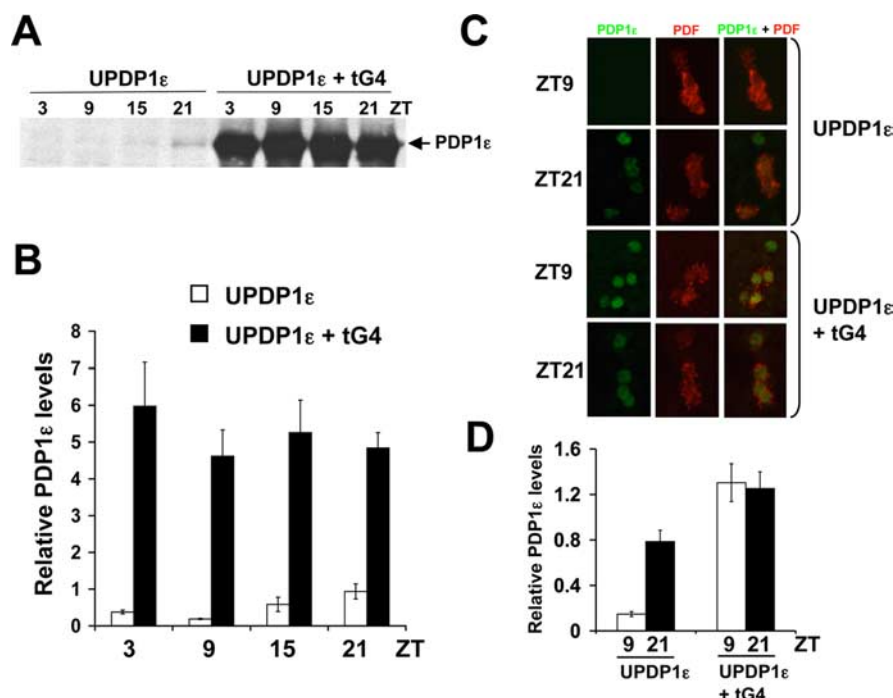Cycling of *Clk* mRNA in UPDP1ε+*tim*Gal4 flies suggests that

Figure 3. Overexpression of PDP1e in oscillator cells. **A**, Western blot of head extracts from w;UAS-PDP1ε/+;+/+ (UPDP1ε) and w;UAS-PDP1ε/+;timGal4/+ (UPDP1ε + tG4) flies collected at the indicated times under LD conditions and probed with PDP1 antibody. **B**, Quantification of PDP1ε levels in **A** and at least four independent repeats using three different UAS-PDP1ε inserts. PDP1ε levels were quantified as described in Materials and Methods. **C**, Brains dissected from UPDP1ε + tG4 and control UPDP1ε flies collected at ZT9 and ZT21 were probed with PDP1 and PDF antibodies. A representative 1 μm optical section of sLN$_v$s is visualized for PDP1 (left panels), PDF (middle panels), or PDP1 plus PDF (right panels). **D**, PDP1 immunostaining in UPDP1ε + tG4 and control UPDP1ε flies was quantified as the ratio of PDP1/PDF staining. Staining in sLN$_v$s was quantified from at least four brains (i.e., at least 2 brains from 2 independent experiments).
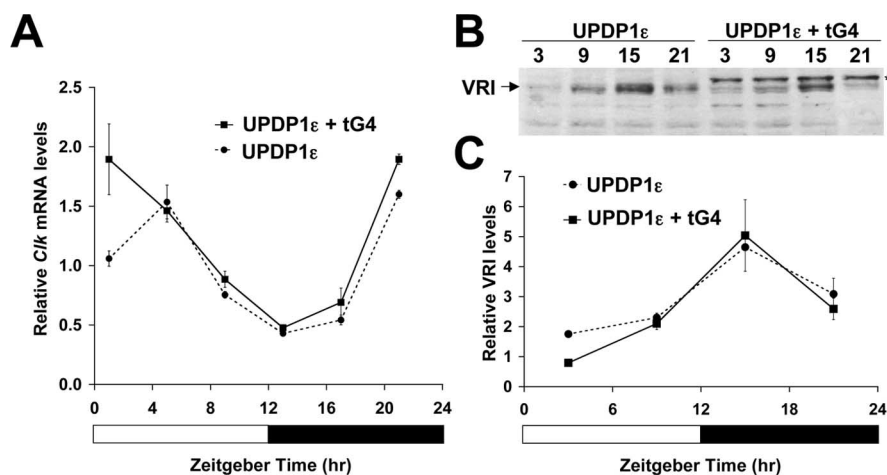

Figure 4. Overexpression of PDP1ε in oscillator cells does not disrupt *Clk* mRNA or VRI cycling. **A**, qPCR of *Clk* mRNA from the heads of w;UAS-PDP1ε/+;UAS-PDP1ε/+ (UPDP1ε) and w; UAS-PDP1ε/+;UAS-PDP1ε/timGal4 (UPDP1ε + tG4) flies collected at the indicated times under LD conditions (ZT). Relative *Clk* mRNA levels were quantified as described in Materials and Methods. The black and white bars represent times when lights were on or off, respectively. **B**, Western blot of head extracts from UPDP1ε and UPDP1ε + tG4 flies collected at the indicated times under LD conditions and probed with VRI antibody. The asterisk denotes the PDP1ε band that did not wash off completely from the blot in Figure 3A. **C**, Quantification of VRI levels in the Western blot in **B** and at least two independent repeats. VRI levels were quantified as described in Materials and Methods.

the circadian oscillator is functional and predicts that VRI should cycle in the opposite phase as *Clk* mRNA (Cyran et al., 2003; Glossop et al., 2003). To determine whether this is the case, VRI levels were measured in UPDP1ε + timGal4 and control UPDP1ε flies under LD conditions. The same blot used to show that

PDP1ε was overexpressed in UPDP1ε + timGal4 flies (Fig. 3A) was reprobed with VRI antiserum to reveal a rhythm in VRI levels similar to that in control flies (Fig. 4B,C). Peak levels of VRI coincided with trough levels of *Clk* mRNA, as would be expected given that VRI represses *Clk* transcription (Cyran et al., 2003; Glossop et al., 2003). These data also confirm that UPDP1ε + timGal4 flies contain a functional circadian oscillator.

Constant high or low PDP1ε levels disrupt behavioral rhythms without disrupting oscillator function in brain pacemaker neurons

Given that constant high or constant low levels of PDP1ε had little or no effect on circadian oscillator function, we expected that altered PDP1ε levels would not affect locomotor activity rhythms. Locomotor activity of flies expressing constant low (2xUAS-PDP1i + timGal4, 2xUAS-PDP1i + pdfGal4) or high (2xUAS-PDP1ε + timGal4, 2xUAS-PDP1ε + pdfGal4) PDP1ε levels was measured along with control (2xUAS-PDP1i, 2xUAS-PDP1ε, timGal4, and pdfGal4) flies under DD conditions after 3 d of entrainment in LD cycles. Surprisingly, only ~17% of flies expressing constant low levels of PDP1ε in clock cells (i.e., 2xUAS-PDP1i + timGal4) displayed rhythms in locomotor activity compared with ~78% of UAS-PDP1i transgene only and ~80% of timGal4 driver only control flies (Table 1). Rhythmic 2xUAS-PDP1i + timGal4 flies had long period rhythms with a lower power than controls. Overall activity was somewhat lower in 2xUAS-PDP1i + timGal4 flies than w and timGal4 controls, whereas 2xUAS-PDP1i controls had anomalously high levels of activity. When PDP1i expression was restricted to LN$_v$s using the pdfGal4 driver (i.e., 2xUAS-PDP1i + pdfGal4), locomotor activity rhythms were abolished, whereas ~57% of control pdfGal4 flies displayed rhythmic locomotor activity (Table 1). Overall activity of 2xUAS-PDP1i + pdfGal4 flies was comparable to 2xUAS-PDP1i + timGal4 flies.

PDP1ε overexpression also disrupted locomotor activity rhythms. Only ~12% of flies that constantly overexpress PDP1ε in all clock cells (i.e., 2xUAS-PDP1ε + timGal4) exhibited rhythmic locomotor activity compared with ~74% of 2xUAS-PDP1ε flies and 100% of timGal4 flies (Table 1). Restricting PDP1ε expression to LN$_v$s using pdfGal4 resulted in ~10% of flies having rhythmic locomotor activity versus ~95% of pdfGal4 control flies (Table 1). The power of rhythmic 2xUAS-PDP1ε + timGal4 and 2xUAS-PDP1ε + pdfGal4 flies was lower than 2xUAS-PDP1ε, tim-

Gal4, and *w* controls. Overall activity levels in 2xUAS-PDP1ε+*tim*Gal4 and 2xUAS-PDP1ε+*pdf*Gal4 flies was similar to *w*, *tim*Gal4, and *pdf*Gal4 flies, whereas 2xUAS-PDP1ε flies had anomalously high activity levels. These results demonstrate that constant high or low levels of PDP1ε severely disrupt locomotor activity rhythms. However, circadian oscillator function persists in flies with constant high or low PDP1ε levels, which suggests that PDP1ε affects locomotor activity rhythms as an output of the circadian clock rather than as a component of the clock.

Although the circadian oscillator continues to operate in fly heads when PDP1ε is constantly high or low, this does not necessarily mean that circadian oscillators are functioning in the pacemaker cells that control locomotor activity rhythms because photoreceptors represent >80% of circadian oscillators in fly heads (Glossop and Hardin, 2002). To determine whether flies expressing constant low levels of PDP1ε have functional LN$_v$ oscillators, the abundance of TIM was assessed in LN$_v$s via immunostaining. UAS-PDP1i+*tim*Gal4 and control *w* flies were entrained to LD cycles and collected at CT21 and CT9 on the second day of DD. Brains from these flies were dissected and probed with antisera against TIM and the LN$_v$ marker PDF and imaged via confocal microscopy. In both 2xUAS-PDP1i+*tim*Gal 4 and control *w* brains, the intensity of TIM immunofluorescence was high at CT21 and low at CT9 in LN$_v$s (Fig. 5). To assess LN$_v$ oscillator function in flies expressing constant high levels of PDP1ε, 2xUAS-PDP1ε+*tim*Gal4 and control *w* flies were entrained to LD cycles and collected at CT1 and CT13 on the second day of DD. Brains from these flies were dissected and probed with antisera against PER and PDF and imaged via confocal microscopy. In both 2xUAS-PDP1ε+*tim*Gal4 and control *w* brains, the intensity of PER immunofluorescence was high at CT1 and low at CT13 in LN$_v$s (Fig. 6). Rhythmic expression of TIM and PER in LN$_v$s from 2xUAS-PDP1i+*tim*Gal 4 and 2xUAS-PDP1ε+*tim*Gal4 flies, respectively, demonstrates that locomotor activity pacemaker neurons contain functional circadian oscillators.

Because some behaviorally arrhythmic clock gene variants show molecular rhythmicity over the first 2 d in DD, TIM and PER cycling were assayed in the LN$_v$s of flies expressing reduced or increased levels of PDP1ε in clock cells during day 5 in DD. Rhythmic TIM immunofluorescence

Table 1. Reducing and increasing PDP1ε levels disrupt locomotor activity rhythms

Genotype	Percentage rhythmic (n)	Period (h) ± SEM	Power ± SEM	Activity ± SEM
w;+/+;+/+	75.0 (172)	23.8 ± 0.03	78.9 ± 3.7	17.8 ± 0.6
w;+/+;*tim*-Gal4/+	80.5 (41)	24.6 ± 0.07	76.7 ± 5.4	16.7 ± 0.9
w;+/+;*pdf*-Gal4/+	57.0 (35)	24.2 ± 0.13	68.7 ± 7.7	14.0 ± 0.8
w;PDP1iA/+; w;PDP1iB/+	77.8 (38)	23.4 ± 0.08	72.8 ± 5.3	28.3 ± 2.1
w;PDP1iA/+; w;PDP1iB/*tim*-Gal4	17.2 (29)	25.3 ± 0.23	35.3 ± 1.7	13.5 ± 1.0
w;PDP1iA/+; w;PDP1iB/*pdf*-Gal4	0 (27)	n.a.	n.a.	12.1 ± 0.7
w;+/+;+/+	96.0 (25)	23.5 ± 0.15	96.1 ± 6.4	19.9 ± 2.3
w;+/+;*tim*-Gal4/+	100.0 (31)	24.3 ± 0.15	78.4 ± 5.2	21.6 ± 2.0
w;+/+;*pdf*-Gal4/+	95.5 (22)	24.3 ± 0.09	76.4 ± 9.5	13.5 ± 2.3
w;PDP1εA/+; w;PDP1εB/+	73.9 (29)	24.5 ± 0.16	78.1 ± 11.7	27.1 ± 3.9
w;PDP1εA/+; w;PDP1εB/*tim*-Gal4	9.7 (31)	25.2 ± 0.12	24.5 ± 5.9	15.4 ± 1.8
w;PDP1εA/+; w;PDP1εB/*pdf*-Gal4	10.3 (29)	24.1 ± 0.02	27.2 ± 2.3	19.1 ± 1.5

Period and power were calculated for all rhythmic animals as described in Materials and Methods. Activity was calculated for all flies that survived to the end of the experiment, as described in Materials and Methods. n.a., Not applicable.
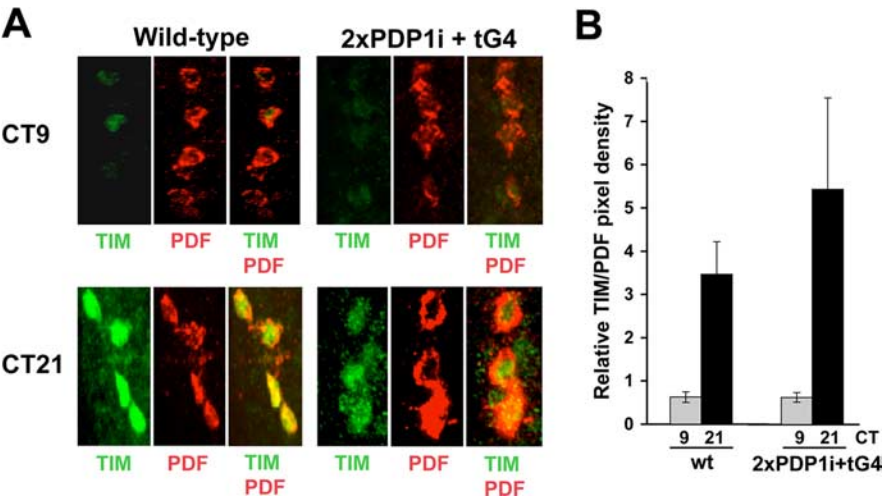

Figure 5. PDP1 RNAi does not disrupt TIM cycling in sLN$_v$s during DD. ***A***, Brains dissected from wild-type and *w*;UAS-PDP1iA/ UAS-PDP1iB;*tim*Gal4/+ (2xPDP1i+tG4) flies collected during the second day of DD at CT9 and CT21 were probed with TIM and PDF antibodies. A representative 1 μm optical section of sLN$_v$s is visualized for TIM (left panels), PDF (middle panels), or TIM plus PDF (right panels). TIM (green) and PDF (red) coimmunostaining is visualized as yellow. ***B***, TIM levels in control 2xPDP1i and 2xPDP1i+tG4 flies was quantified as the ratio of TIM/PDF immunostaining. Staining in sLN$_v$s was quantified from at least 12 brains (i.e., at least 4 brains from 3 independent experiments). wt, Wild type.
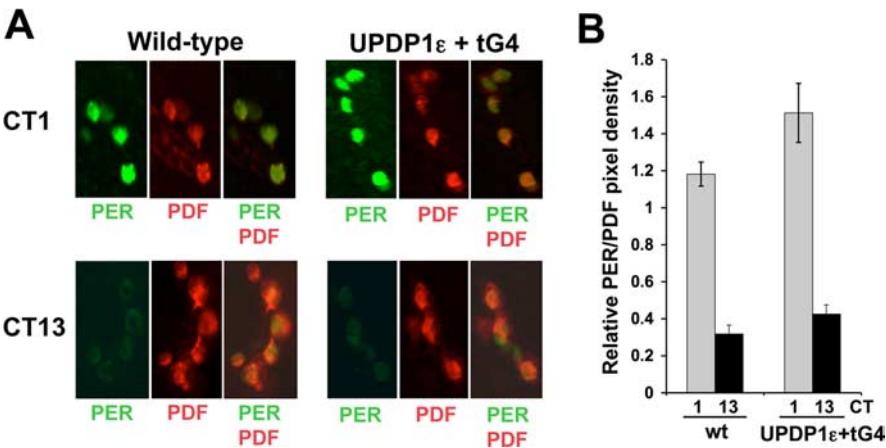

Figure 6. PDP1ε overexpression does not disrupt PER cycling in sLN$_v$s during DD. ***A***, Brains dissected from wild-type and *w*;UAS-PDP1ε/+;UAS-PDP1ε/*tim*Gal4 (UPDP1ε+tG4) flies collected during the second day of DD at CT1 and CT13 were probed with PER and PDF antibodies. A representative 1 μm optical section of sLN$_v$s is visualized for PER (left panels), PDF (middle panels), or PER plus PDF (right panels). PER (green) and PDF (red) coimmunostaining is visualized as yellow. ***B***, PER immunostaining in wild-type (wt) and UPDP1ε+tG4 flies was quantified as the ratio of PER/PDF staining. Staining in sLN$_v$s was quantified from at least 12 brains (i.e., at least 4 brains from 3 independent experiments).

in the LN_vs of flies expressing constant low levels of PDP1ε (2xUAS-PDP1i+timGal4) is similar to that seen in 2xUAS-PDP1i controls on day 5 of DD (supplemental Fig. 1*A,B*, available at www.jneurosci.org as supplemental material). Likewise, rhythmic PER immunofluorescence in the LN_vs of flies expressing constant high levels of PDP1ε (UPDP1ε+timGal4) is similar to that seen in UPDP1ε controls on day 5 of DD (supplemental Fig. 1*C,D*, available at www.jneurosci.org as supplemental material). These results demonstrate that the circadian oscillator continues to function at a time when behavioral rhythmicity is lost.

The loss of rhythmic behavior in 2xUAS-PDP1i+timGal4 and UPDP1ε+timGal4 flies suggests that PDP1ε either controls rhythmic transcription of clock output genes or is necessary for the development of sLN_vs. PDP1ε, like other PDP1 isoforms, is expressed in embryos and larvae (Reddy et al., 2000). A *Pdp1* null mutant, $Pdp1^{P205}$, causes developmental arrest during the larval stage, indicating that *Pdp1* plays an essential role during larval development (Cyran et al., 2003; Reddy et al., 2006). We have shown that sLN_vs are present in flies expressing constant low or high levels of PDP1ε (Figs. 1, 3). However, it is possible that behavioral arrhythmicity results from missing or defective sLN_v projections in 2xUAS-PDP1i+timGal4 and UPDP1ε+timGal4 flies. To investigate this possibility, projections from the sLN_vs were visualized using antisera against pigment dispersing factor (PDF), a neuropeptide that is necessary for behavioral rhythmicity (Renn et al., 1999).

The sLN_vs from all 2xUAS-PDP1i+timGal4 (*n* = 22 brain hemispheres) and control 2xUAS-PDP1i (*n* = 8 brain hemispheres) flies extend projections into the dorsal protocerebrum (supplemental Fig. 2*A,B*, available at www.jneurosci.org as supplemental material). Projections in 2xUAS-PDP1i+timGal4 flies were similar in morphology to those of 2xUAS-PDP1i controls in all but two cases: one projection split and then reunited, and one projection was overextended (supplemental Fig. 2*C*, available at www.jneurosci.org as supplemental material; and data not shown). Likewise, all projections from the sLN_vs of UPDP1ε+timGal4 (*n* = 12 brain hemispheres) and control UPDP1ε (*n* = 8 brain hemispheres) flies extend into the dorsal protocerebrum (supplemental Fig. 2*D,E*, available at www. jneurosci.org as supplemental material). UPDP1ε+timGal4 and control UPDP1ε sLN_v projections were similar in morphology with two exceptions: one UPDP1ε projection split and then reunited, and one UPDP1ε+timGal4 projection was overextended (supplemental Fig. 2*F*, available at www.jneurosci.org as supplemental material; and data not shown). These results demonstrate that constant low or high PDP1ε levels have little affect on the morphology of sLN_v projections. Given that a single dorsally projecting sLN_v is sufficient to mediate behavioral rhythms (Helfrich-Forster, 1998), these data argue that behavioral arrhythmicity in 2xUAS-PDP1i+timGal4 and UPDP1ε+timGal4 flies is attributable to the disruption of rhythmic output gene transcription.

Discussion

PDP1ε is not necessary for circadian oscillator function

Transcriptional activation by PDP1ε and repression by VRI are thought to mediate *Clk* mRNA cycling (Cyran et al., 2003). Both VRI and PDP1ε bind to V/P-boxes, and the ratio of VRI to PDP1ε binding is thought to control *Clk* mRNA cycling such that a high VRI/PDP1ε ratio during the late day and early evening represses *Clk* transcription and a low VRI/PDP1ε ratio from mid evening to early morning activates *Clk* transcription (Cyran et al., 2003). Because VRI levels peak during the early evening and

PDP1ε levels peak late in the evening (Cyran et al., 2003; Glossop et al., 2003), V/P-box binding and *Clk* transcription are directly related to the levels of VRI and PDP1ε.

Because *Pdp1ε* and *vri* are activated by CLK-CYC (Blau and Young, 1999; Cyran et al., 2003), it follows that *Clk* mRNA should be constantly low in a *Clk* or *cyc* mutant because of low PDP1ε levels, yet constant high levels of *Clk* mRNA are seen (Glossop et al., 1999). This result might suggest that a low level of PDP1ε can fully activate *Clk* when VRI levels are low (Cyran et al., 2003). The complete loss of all PDP1 isoforms in homozygous $Pdp1^{P205}$ larvae eliminates *Clk* expression, indicating that PDP1ε activates *Clk* transcription (Cyran et al., 2003). However, the lack of *Clk* expression in $Pdp1^{P205}$ mutant larvae may also be attributable to developmental defects that damage or eliminate clock brain neurons, because $Pdp1^{P205}$ mutants are developmentally delayed and rarely survive beyond the third larval instar (Cyran et al., 2003). To avoid potential developmental problems arising from the loss of all PDP1 isoforms expressed in different tissues, we altered PDP1ε levels specifically in clock cells.

If rhythms in the ratio of VRI/PDP1ε are required for *Clk* mRNA cycling, we reasoned that constant low or high levels of PDP1ε would chronically increase or decrease the VRI/PDP1ε ratio, respectively, and the resulting changes in *Clk* mRNA levels would disrupt *Clk* mRNA cycling. However, we found that neither constant low or constant high levels of PDP1ε disrupted *Clk* mRNA cycling (Figs. 2*A*, 4*A*). When PDP1ε levels in oscillator cells were constantly low, the amplitude of *Clk* mRNA cycling was similar to that in timGal4 controls and wild-type flies (Fig. 2*A*) (Bae et al., 1998; Darlington et al., 1998). This conclusion is also supported by PDP1ε overexpression, in which ~10-fold higher levels of PDP1ε in oscillator cells alter neither the overall level of *Clk* mRNA nor the amplitude of *Clk* mRNA cycling (Fig. 4*A*). Comparable levels of *Clk* mRNA in flies expressing low or high levels of PDP1ε in oscillator cells suggest that PDP1ε does not activate *Clk* transcription. However, we cannot discount some role for PDP1ε in activating *Clk* transcription because PDP1ε is not completely eliminated in 2xUAS-PDP1i+timGal4 flies, PDP1ε may constantly be at saturating levels in 2xUAS-PDP1ε+timGal4 flies, and *Clk* mRNA is at lower levels in 2xUAS-PDP1i+timGal4 flies versus timGal4 controls just after dawn.

VRI is known to repress *Clk* transcription *in vivo* (Cyran et al., 2003; Glossop et al., 2003). Because *Clk* mRNA continues to cycle when PDP1ε levels are high or low, VRI levels would be predicted to cycle with peak levels coincident with the trough in *Clk* mRNA abundance. Indeed, VRI levels cycle robustly in both 2xUAS-PDP1i+timGal4 and 2xUAS-PDP1ε+timGal4 flies (Figs. 2*B,C*, 4*B,C*). This result not only reinforces the role of VRI as a *Clk* repressor but provides additional evidence that the molecular feedback loops that underlie the circadian oscillator are operating normally.

PDP1ε is required for behavioral rhythmicity

The circadian oscillator is thought to control overt physiological, metabolic, and behavioral rhythms via rhythmically transcribed "output" genes. Microarray analyses of fly heads demonstrate that >100 transcripts are rhythmically expressed and that the vast majority of these transcripts represent clock output genes rather than oscillator components (Claridge-Chang et al., 2001; McDonald and Rosbash, 2001; Ceriani et al., 2002; Lin et al., 2002; Ueda et al., 2002; Wijnen et al., 2006). Some of these output transcripts appear to be directly controlled by CLK-CYC (McDonald and Rosbash, 2001), but their roles in regulating overt
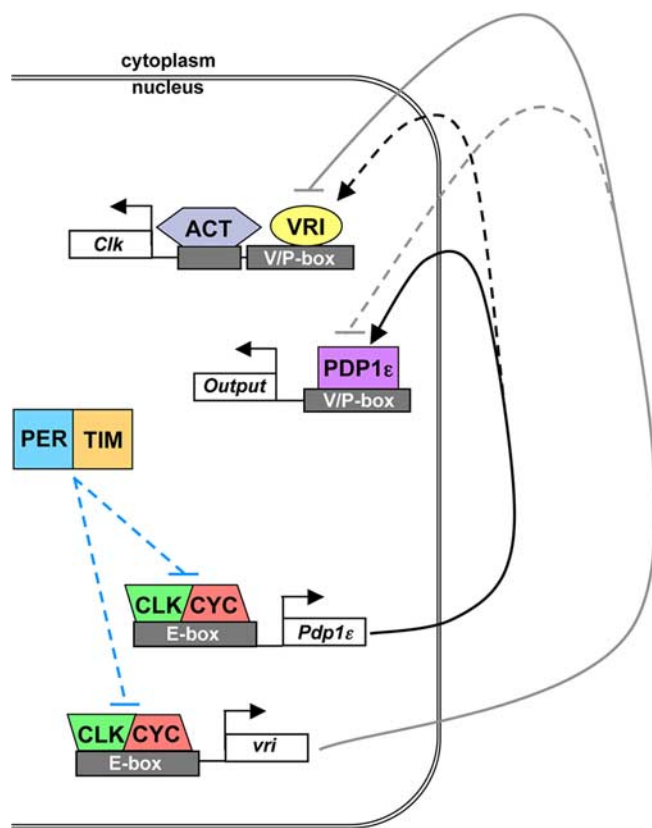
Figure 7. Model for the function of PDP1ε. CLK-CYC heterodimers bind E-boxes to activate *vri* and *Pdp1ε* transcription. VRI accumulates in concert with its mRNA and binds V/P-boxes to inhibit *Clk* transcription (solid gray line). PDP1ε accumulates to peak levels several hours after VRI, activates output genes required for behavioral activity (solid black line), and possibly counteracts VRI inhibition (dashed black line). VRI may also contribute to rhythmic output gene transcription (dashed gray line). PER-TIM accumulates in parallel with PDP1ε and inhibits CLK-CYC-dependent transcription of *vri* and *Pdp1ε* (dashed blue line), thereby removing VRI inhibition of *Clk* transcription. An activator of *Clk* transcription (ACT) is constantly present, thus accounting for high levels of *Clk* mRNA in *Clk*^{Jrk} and *cyc*^{01} mutants and in wild-type flies when VRI is absent.

rhythms have not been characterized. A key property of clock output genes is that circadian oscillator function persists in their absence. Perhaps the best example of a clock output gene is the neuropeptide PDF which, when eliminated, has no effect on circadian oscillator function but abolishes locomotor activity rhythms (Renn et al., 1999). However, *pdf* is not rhythmically transcribed, although its expression in sLN$_v$s is dependent on *Clk* and *cyc* (Park et al., 2000). In fact, we do not know of any rhythmically expressed output genes that control specific physiological, metabolic, or behavioral rhythms.

Our analysis indicates that *Pdp1ε* is the first rhythmically expressed output gene that is required to mediate an overt circadian rhythm. Rhythmic transcription of *Pdp1ε* is directly controlled by CLK-CYC (Cyran et al., 2003), and constant low or high levels of PDP1ε have little effect on *Clk* mRNA cycling or circadian oscillator function in sLN$_v$s (Figs. 1–4) but severely impair behavioral rhythmicity (Table 1). The vast majority of flies expressing constant low or high levels of PDP1ε in oscillator cells extend morphologically normal sLN$_v$ projections in at least one (and typically both) brain hemisphere, which indicates that behavioral arrhythmicity is not attributable to defects in sLN$_v$ development (supplemental Fig. 2, available at www.jneurosci.org as supplemental material). Because PDP1ε is a rhythmically expressed

bZIP transcriptional factor, we favor the possibility that PDP1ε mediates behavioral rhythms by rhythmically activating effector genes (Fig. 7). These second-order rhythmic transcripts may represent some of those identified in previous microarray studies, the abundance of which peaks near dawn (Claridge-Chang et al., 2001; McDonald and Rosbash, 2001; Ceriani et al., 2002; Lin et al., 2002; Ueda et al., 2002; Wijnen et al., 2006). In fact, it is possible that PDP1ε controls many second-order rhythmic transcripts and, consequently, other overt rhythms. Likewise, VRI may also contribute to overt rhythmicity by regulating clock output genes (Fig. 7). The extent to which PDP1ε and/or VRI control rhythmic transcripts that mediate physiological, metabolic, and behavioral rhythms awaits future study.

PDP1ε is related to three rhythmically expressed PAR domain-containing bZIP transcriptional activators in mammals: albumin gene site D-binding protein (DBP), thyroid embryonic factor, and hepatocyte leukemia factor (Wuarin and Schibler, 1990; Falvey et al., 1995; Fonjallaz et al., 1996). DBP knock-out mice show lower levels of locomotor activity and a shorter circadian period than wild-type animals, yet robust circadian oscillator function persists (Lopez-Molina et al., 1997). These results suggest that DBP functions to control clock output, consistent with the function of PDP1ε in flies. DBP binds to the same regulatory element as adenovirus E4 promoter ATF site-binding protein (E4BP4), a rhythmically expressed bZIP repressor that is related to VRI (Mitsui et al., 2001). Because E4BP4 is expressed in the opposite phase as DBP (Mitsui et al., 2001), sequential binding of E4BP4 and DBP could control rhythmic target gene transcription. Given that VRI and PDP1ε bind the same target sequence in flies, antagonistic binding of PAR domain transcription factors and their repressors could be a conserved mechanism for controlling rhythmic outputs.

References

Bae K, Lee C, Sidote D, Chuang KY, Edery I (1998) Circadian regulation of a *Drosophila* homolog of the mammalian Clock gene: PER and TIM function as positive regulators. Mol Cell Biol 18:6142–6151.

Blau J, Young MW (1999) Cycling *vrille* expression is required for a functional *Drosophila* clock. Cell 99:661–671.

Brand AH, Perrimon N (1993) Targeted gene expression as a means of altering cell fates and generating dominant phenotypes. Development 118:401–415.

Ceriani MF, Hogenesch JB, Yanovsky M, Panda S, Straume M, Kay SA (2002) Genome-wide expression analysis in *Drosophila* reveals genes controlling circadian behavior. J Neurosci 22:9305–9319.

Claridge-Chang A, Wijnen H, Naef F, Boothroyd C, Rajewsky N, Young MW (2001) Circadian regulation of gene expression systems in the *Drosophila* head. Neuron 32:657–671.

Cyran SA, Buchsbaum AM, Reddy KL, Lin MC, Glossop NR, Hardin PE, Young MW, Storti RV, Blau J (2003) *vrille*, Pdp1, and *dClock* form a second feedback loop in the *Drosophila* circadian clock. Cell 112:329–341.

Darlington TK, Wager-Smith K, Ceriani MF, Staknis D, Gekakis N, Steeves TD, Weitz CJ, Takahashi JS, Kay SA (1998) Closing the circadian loop: CLOCK-induced transcription of its own inhibitors *per* and *tim*. Science 280:1599–1603.

Emery P, So WV, Kaneko M, Hall JC, Rosbash M (1998) CRY, a *Drosophila* clock and light-regulated cryptochrome, is a major contributor to circadian rhythm resetting and photosensitivity. Cell 95:669–679.

Falvey E, Fleury-Olela F, Schibler U (1995) The rat hepatic leukemia factor (HLF) gene encodes two transcriptional activators with distinct circadian rhythms, tissue distributions and target preferences. EMBO J 14:4307–4317.

Fonjallaz P, Ossipow V, Wanner G, Schibler U (1996) The two PAR leucine zipper proteins, TEF and DBP, display similar circadian and tissue-specific expression, but have different target promoter preferences. EMBO J 15:351–362.

Glossop NR, Hardin PE (2002) Central and peripheral circadian oscillator mechanisms in flies and mammals. J Cell Sci 115:3369–3377.

Glossop NR, Lyons LC, Hardin PE (1999) Interlocked feedback loops within the *Drosophila* circadian oscillator. Science 286:766–768.

Glossop NR, Houl JH, Zheng H, Ng FS, Dudek SM, Hardin PE (2003) VRILLE feeds back to control circadian transcription of *Clock* in the *Drosophila* circadian oscillator. Neuron 37:249–261.

Grumbling G, Strelets V (2006) FlyBase: anatomical data, images and queries. Nucleic Acids Res 34:D484–D488.

Hardin PE (2004) Transcription regulation within the circadian clock: the E-box and beyond. J Biol Rhythms 19:348–360.

Hardin PE (2005) The circadian timekeeping system of *Drosophila*. Curr Biol 15:R714–R722.

Hardin PE, Hall JC, Rosbash M (1990) Feedback of the *Drosophila period* gene product on circadian cycling of its messenger RNA levels. Nature 343:536–540.

Hazelrigg T, Levis R, Rubin GM (1984) Transformation of white locus DNA in *Drosophila*: dosage compensation, zeste interaction, and position effects. Cell 36:469–481.

Helfrich-Forster C (1998) Robust circadian rhythmicity of *Drosophila melanogaster* requires the presence of lateral neurons: a brain-behavioral study of *disconnected* mutants. J Comp Physiol A Neuroethol Sens Neural Behav Physiol 182:435–453.

Houl JH, Yu W, Dudek SM, Hardin PE (2006) *Drosophila* CLOCK is constitutively expressed in circadian oscillator and non-oscillator Cells. J Biol Rhythms 21:93–103.

Hunter-Ensor M, Ousley A, Sehgal A (1996) Regulation of the *Drosophila* protein *timeless* suggests a mechanism for resetting the circadian clock by light. Cell 84:677–685.

Konopka RJ, Benzer S (1971) Clock mutants of *Drosophila melanogaster*. Proc Natl Acad Sci USA 68:2112–2116.

Lee C, Bae K, Edery I (1999) PER and TIM inhibit the DNA binding activity of a *Drosophila* CLOCK-CYC/dBMAL1 heterodimer without disrupting formation of the heterodimer: a basis for circadian transcription. Mol Cell Biol 19:5316–5325.

Lin Y, Han M, Shimada B, Wang L, Gibler TM, Amarakone A, Awad TA, Stormo GD, Van Gelder RN, Taghert PH (2002) Influence of the *period*-dependent circadian clock on diurnal, circadian, and aperiodic gene expression in *Drosophila melanogaster*. Proc Natl Acad Sci USA 99:9562–9567.

Lopez-Molina L, Conquet F, Dubois-Dauphin M, Schibler U (1997) The DBP gene is expressed according to a circadian rhythm in the suprachiasmatic nucleus and influences circadian behavior. EMBO J 16:6762–6771.

McDonald MJ, Rosbash M (2001) Microarray analysis and organization of circadian gene expression in *Drosophila*. Cell 107:567–578.

Mitsui S, Yamaguchi S, Matsuo T, Ishida Y, Okamura H (2001) Antagonistic role of E4BP4 and PAR proteins in the circadian oscillatory mechanism. Genes Dev 15:995–1006.

Myers MP, Wager-Smith K, Rothenfluh-Hilfiker A, Young MW (1996) Light-induced degradation of TIMELESS and entrainment of the *Drosophila* circadian clock. Science 271:1736–1740.

Park JH, Helfrich-Forster C, Lee G, Liu L, Rosbash M, Hall JC (2000) Differential regulation of circadian pacemaker output by separate clock genes in *Drosophila*. Proc Natl Acad Sci USA 97:3608–3613.

Reddy KL, Wohlwill A, Dzitoeva S, Lin MH, Holbrook S, Storti RV (2000) The *Drosophila PAR domain protein* 1 (*Pdp1*) gene encodes multiple differentially expressed mRNAs and proteins through the use of multiple enhancers and promoters. Dev Biol 224:401–414.

Reddy KL, Rovani MK, Wohlwill A, Katzen A, Storti RV (2006) The *Drosophila Par domain protein I gene, Pdp1*, is a regulator of larval growth, mitosis and endoreplication. Dev Biol 289:100–114.

Renn SC, Park JH, Rosbash M, Hall JC, Taghert PH (1999) A *pdf* neuropeptide gene mutation and ablation of PDF neurons each cause severe abnormalities of behavioral circadian rhythms in *Drosophila*. Cell 99:791–802.

Rutila JE, Suri V, Le M, So WV, Rosbash M, Hall JC (1998) CYCLE is a second bHLH-PAS clock protein essential for circadian rhythmicity and transcription of *Drosophila period* and *timeless*. Cell 93:805–814.

Sehgal A, Rothenfluh-Hilfiker A, Hunter-Ensor M, Chen Y, Myers MP, Young MW (1995) Rhythmic expression of *timeless*: a basis for promoting circadian cycles in *period* gene autoregulation. Science 270:808–810.

Tanoue S, Krishnan P, Krishnan B, Dryer SE, Hardin PE (2004) Circadian clocks in antennal neurons are necessary and sufficient for olfaction rhythms in *Drosophila*. Curr Biol 14:638–649.

Ueda HR, Matsumoto A, Kawamura M, Iino M, Tanimura T, Hashimoto S (2002) Genome-wide transcriptional orchestration of circadian rhythms in *Drosophila*. J Biol Chem 277:14048–14052.

Wijnen H, Naef F, Boothroyd C, Claridge-Chang A, Young MW (2006) Control of daily transcript oscillations in *Drosophila* by light and the circadian clock. PLoS Genet 2:e39.

Wuarin J, Schibler U (1990) Expression of the liver-enriched transcriptional activator protein DBP follows a stringent circadian rhythm. Cell 63:1257–1266.

Yu W, Zheng H, Houl JH, Dauwalder B, Hardin PE (2006) PER-dependent rhythms in CLK phosphorylation and E-box binding regulate circadian transcription. Genes Dev 20:723–733.